**OPEN**

# A non-invasive imaging for the *in vivo* tracking of high-speed vesicle transport in mouse neutrophils

Kenji Kikushima, Sayaka Kita & Hideo Higuchi

Department of Physics, Graduate School of Science, The University of Tokyo, 7-3-1 Bunkyo-ku, Tokyo 113-0033, Japan.

**Neutrophils play an essential role in the innate immune response. To understand neutrophil activity, the development of a new technique to observe neutrophils *in situ* is required. Here, we report the development of a non-invasive technique for the *in vivo* imaging of neutrophils labeled with quantum dots, up to 100 μm below the skin surface of mice. Upon inflammation neutrophils began to extravasate from blood vessels and locomoted in interstitial space. Most intriguingly, the quantum dots were endocytosed into vesicles in the neutrophils, allowing us to track the vesicles at 12.5 msec/frame with 15–24 nm accuracy. The vesicles containing quantum dots moved as "diffuse-and-go" manner and were transported at higher speed than the *in vitro* velocity of a molecular motor such as kinesin or dynein. This is the first report in which non-invasive techniques have been used to visualize the internal dynamics of neutrophils.**

N eutrophils are the most abundant type of white blood cell and are important in innate immunity and the acute inflammatory response. Upon inflammation or bacterial invasion, cytokines are produced in the regions surrounding the inflammation. These signals recruit neutrophils to the site of inflammation via their extravasation from blood vessels[1–3]. Despite progress in genetic engineering techniques, experiments with neutrophils have been remained difficult because neutrophils have a short life span and do not grow or differentiate *in vitro*. Neutrophil-like cell lines have been investigated for cell-based biological studies; however, the motility of these cells is often distinct from that of primary neutrophils *in vivo*.

Previous studies detailing the *in vivo* imaging of neutrophils have used mice in which the EGFP gene was inserted into the lysozyme M locus, resulting in the specific labeling of neutrophils and macrophages[4]. Two-photon microscopy allowed for the investigation of the collective behaviors of the EGFP-expressing neutrophils *in vivo* in response to bacterial infection or injury after the dissection of draining lymph nodes[5] or thoracotomy[6]. These observations clearly revealed interactions between neutrophils and macrophages. However, with two-photon microscopy, the fluorophores are excited by only a small number of photons, and the images are captured using single-spot scanning. Therefore, the images of two-photon microscopy are darker than that of spinning-disk confocal microscopy using multi-spot scanning, and longer sampling time is required to collect enough fluorescence photons. Moreover, the fluorescence is strongly scattered and absorbed by the epidermis and cortex. Therefore, surgery is needed to remove the offending tissues and to obtain sufficient fluorescence. However, the surgery itself activates inflammatory signals. Therefore, it has been difficult to maintain non-inflammatory, physiological conditions while performing these types of studies.

A wide variety of factors are required for neutrophils to exert their bactericidal function, including various cytokines, proteinases, bactericidal proteins, nitric oxide, reactive oxygen species and direct physical interaction with surrounding cells (reviewed in ref. 1, 2, 3). These factors are all intricately related, and while investigations have examined the effects of individual factors on neutrophil activity, a comprehensive understanding of the full *in vivo* mechanism remains elusive. Because it is especially important to preserve these interactions in immunological studies, a non-invasive technique for the *in vivo* observation of neutrophils has been strongly desired.

To perform non-invasive imaging, we searched for molecular markers with bright fluorescence and the corresponding systems to observe the readouts with high sensitivity. Previously, we succeeded in observing the movement of a single monoclonal anti-HER2 antibody in tumor cells *in vivo* using quantum dots (QD)[7]. The *in vivo* imaging of protease-activated receptor-1 (PAR1) dynamics on the cell membrane of a tumor cell was also examined, and the membrane fluidity varied depending on the metastatic state of the tumor[8]. Furthermore, Hamada et al. recently observed the *in vivo* distribution of VEGFR (vascular endothelial growth factor receptor) on the vascular wall[9]. All of these experiments demonstrate the utility of QDs and their desirable properties,

including good photostability and strong fluorescence when compared with conventional organic dyes and fluorescent proteins[10]. Importantly, however, to obtain enough fluorescence from the QDs, surgery was performed in each of these studies.

In this study, we report the non-invasive imaging of neutrophils labeled with QDs in the mouse auricle using a high-contrast imaging system. Intriguingly, the QDs were endocytosed into vesicles in the neutrophils, and we were able to track vesicular movement inside the cell at a frame rate of 12.5 msec/frame (80 frames/sec) with 15 nm accuracy. Upon inflammation, some vesicles moved in a "diffuse-and-go" manner. During the "go" phase, the maximum velocity of the vesicle reached a few times higher than the *in vitro* velocity of a molecular motor, such as kinesin or dynein. The high-speed motility of the vesicles may result from the cooperation of motor proteins, microtubules and actin filaments and might prove to be important for the bactericidal function of neutrophils.

## Results

**Labeling of neutrophils with QD-antibody conjugates.** Mouse Ly6G, a GPI-anchored myeloid differentiation marker also known as Gr1, is expressed specifically on monocytes within the bone marrow and on peripheral neutrophils[11]. Biotinylated anti-Ly6G antibodies were reacted with streptavidin coated QDs to form QD-anti-Ly6G antibody conjugates. Purified neutrophils were mixed with the QD-antibody conjugates to assess the ability of the anti-Ly6G antibody to label neutrophils with QDs. With a ratio of 20 nM QDs to 40 nM antibody, many QDs were bound around the circumference of the neutrophil (Fig. 1a). The QDs did not bind to neutrophils in the absence of antibody. The number of QDs bound to the surface of the cell did not differ significantly even when the concentration of QDs was greater than 5 nM (Fig. 1a–c).
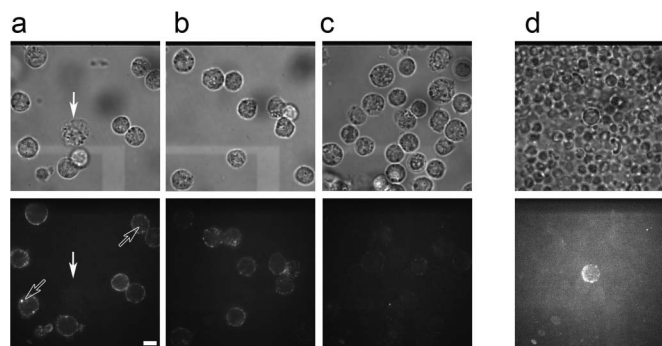


**Figure 1 | Labeling of neutrophils by QD-anti-Ly6G antibody complexes.** (a–c) Neutrophils purified from peritoneal fluid (approximately $10^7$–$10^8$) of ddY mice were incubated with various concentrations of streptavidin coated QDs ((a) 20 nM, (b) 5 nM, (c) 1 nM) and biotinylated anti-Ly6G antibody ((a) 40 nM, (b) 10 nM, (c) 2 nM) in 100 μl PBS for 10 min on ice. After removal of the unbound QDs and antibodies, the QD-labeled neutrophils were observed using transillumination (upper figures) and confocal fluorescent microscopy with 532 nm laser illumination (lower figures). Fluorescent images were captured at 100 msec/frame and averaged over 50 successive images. The brightness and contrast of these fluorescent images (lower figures of (a–c)) were adjusted to similar levels. Transillumination images were not averaged. Monocytes were not labeled by QDs (arrow in (a)). Some QDs were endocytosed and observed inside the neutrophils (open arrows in (a)). (d) Labeling of neutrophils *in vivo* following direct injection of QD-antibody complexes. QDs (330 nM) and the anti-Ly6G antibody (670 nM) in 120 μl PBS were injected into SCID mice via the tail vein. Blood was collected and observed using transillumination (upper figure) and confocal fluorescent microscopy (lower figure). Fluorescent images were captured at 100 msec/frame and averaged over successive ten images. Transillumination images were not averaged. The bar indicates 10 μm.

Monocytes, which could be identified based on their relative size, were not labeled (arrow in Fig. 1a). In addition to the QDs around the surface of the neutrophils, some QDs were internalized by endocytosis and could be observed inside the cells (open arrows in Fig. 1a).

QDs conjugated with anti-neutrophil antibodies were directly injected into the tail vein of SCID mice. The concentration of QDs was approximately 5–20 nM in mouse blood, allowing for the labeling of neutrophils in the peripheral blood with a sufficient number of QDs. Ten minutes after the injection of the QD-antibody conjugates, blood was collected from the heart via cardiac puncture. We confirmed that the QD-antibody conjugates bound only to neutrophils *in vivo* but not to erythrocytes or other cells (Fig. 1d), and we decided to use the methods in all following non-invasive *in vivo* experiments.

**Observation of neutrophils in the mouse auricle under non-invasive conditions.** We developed a high-contrast imaging microscopy equipped with a spinning-disk confocal system (CSU), a fast EMCCD camera, a high power laser, a silicon oil-immersion objective and a stable stage (Fig. 2). We were able to observe blood vessels in the mouse auricle with blue transillumination (400–440 nm) because the mouse auricle is approximately 150 μm thick and hemoglobin strongly absorbs light of this wavelength. Using the microscopy, we succeeded in the non-invasive observation of QD-labeled neutrophils flowing in the auricle blood vessels *in vivo* at a frame rate of 30 msec/frame (Fig. 3, Supplementary Movie 1). These flowing neutrophils were observed over 1 h after injection of the QDs, and the number of neutrophils observed was approximately 4 cells/min. This quantity of neutrophils suggests that the majority of neutrophils in the peripheral blood were observable even considering their density in the peripheral blood and the velocity of blood flow. We were able to observe flowing neutrophils up to 100 μm below the surface of the skin. These results indicate that the direct injection of antibody-conjugated QDs into the tail vein of the mouse is both an easy and effective method for labeling neutrophils *in vivo* and is also useful for the non-invasive observation of leukocytes.

**Effects of inflammation on vascular neutrophil extravasation.** Next, we examined the response of neutrophils to the inflammation induced by 12-O-tetradecanoylphorbol 13-acetate (TPA). In the absence of TPA, the neutrophils in the blood vessel continued to flow and did not stick to the vascular wall, as shown in Figure 3. However, after the induction of inflammation by TPA, the neutrophils began to bind to the wall of the blood vessel (Fig. 4, Supplementary Movies 2 and 3). The neutrophils tended to bind specific portions of the blood vessel wall and formed clusters on the surface. We also observed some neutrophils rolling on the surface of the vessel (upper left in Supplementary Movie 2). Neutrophil rolling is caused by weak binding of the cell to the vascular wall at the beginning of extravasation and in response to inflammation[1-3].

**Tracking of vesicles in neutrophils on the vascular wall.** We occasionally recognized bright fluorescent spots inside the neutrophils on the vascular wall (Fig. 4e,f). These spots were considered to be vesicles containing QDs endocytosed from the cell membrane. The images of the internalized vesicles were captured at 20 msec/frame with a fast EMCCD camera equipped with a CSU unit. Because images of vesicles were not bright enough to track by the FIONA method (fluorescence imaging with one nanometer accuracy[15]), we averaged over successive 5 images in order to make the vesicles brighter than 40 photons/vesicle (Fig. 4f). Averaged profile of intensity of the vesicle was well fitted to two dimensional Gaussian (Fig. 4h). We found that during the recruitment of neutrophils from the peripheral blood to the vascular wall, the vesicles in the neutrophils did not show directional movement but were almost stopped.
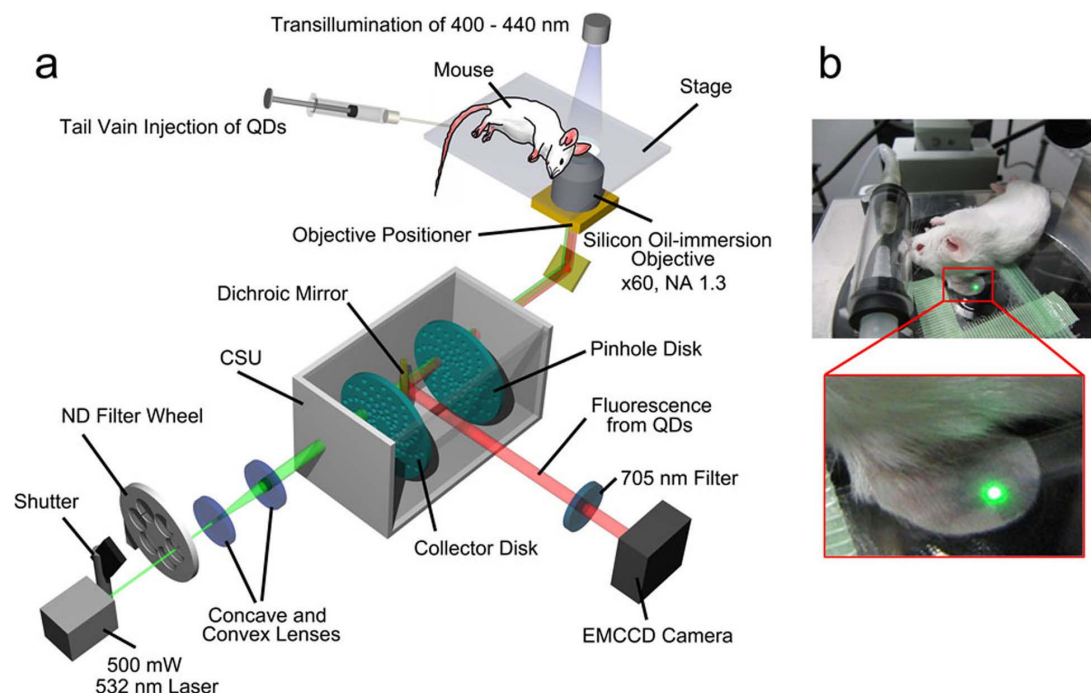
**Figure 2 | Experimental microscopy setup for the non-invasive observation of neutrophils in the mouse auricle.** (a) Mice were anesthetized with 1–3% isoflurane on the stage of the microscope. QD- anti-Ly6G antibody conjugates were injected into the tail vein. The concentration of the QDs in the mouse blood was optimized to be 5–20 nM. The mouse auricle was illuminated by a 500-mW high-power laser at 532 nm. The emission and power of the laser were controlled by a shutter and ND filters. Using a high-NA (NA: 1.3) objective and a CSU system, we obtained high-speed and bright confocal images of the QDs. The $z$-position of the objective was controlled by a piezoelectric actuator, enabling us to obtain 3D images. The fluorescence from the QDs was filtered with a 685–725 nm band-pass filter and captured by an EMCCD camera. Blood vessels in the ear were visualized via transillumination with a 400–440 nm band-pass filter. The transillumination images were not filtered in front of the camera. (b) The mouse ear was put between two glass coverslips and firmly fixed to the stage using adhesive tape.

**High-speed tracking of the vesicles in neutrophils moving in the interstitium.** Twenty-four hours after inducing inflammation, we observed that the neutrophils had extravasated from the blood vessels and migrated to the interstitial tissue outside the blood vessel (Fig. 5 and Supplementary Movie 4). Typically, during the interstitial movement of a neutrophil, the tip of the cell lengthened slowly with diffusive motion. By contrast, the rear portion of the cell simultaneously shrank, which appeared to support the forward movement of the cell body. This manner of migration is consistent with the observed movement of leukocytes in a three-dimensional space, independent of integrin binding[12,13].

Unlike the movement of vesicles in the neutrophils at the vascular wall, the vesicles in the neutrophils moving in the interstitium were actively transported. the movement of these vesicles was captured at 12.5 msec/frame without averaging successive frames and images of their positions were tracked using the FIONA method (Fig. 6). To estimate the accuracy of the tracking, we analyzed amplitude of noise in the traces by following two ways. First, when the movement of a vesicle paused for 1200 ms along the $x$-axis (Vesicle 1, shown in red in the leftmost panel of Fig. 6b), the noise (s.d.) of the $x$-position in the 1200 ms was approximately 15 nm (rightmost panel of Fig. 6b). Second, after low frequency component of translocational Vesicle-1 movement was reduced by 0.3 Hz high-pass filter (Fig. 6c), the average noises during 1 sec in $x$- and $y$-traces of 10 seconds were calculated to be $(x, y) = (21 \pm 3$ nm, $24 \pm 3$ nm$)$ (mean $\pm$ SD, n = 10). This indicates that we were able to measure the position of the vesicle at high speed (12.5 msec/frame), with high positional accuracy (15 nm), non-invasively and *in vivo*.

We were also able to simultaneously track multiple vesicles in a single neutrophil (Fig. 7a,b ; Supplementary Movie 5, Supplementary Fig. S1). The movements of the vesicles were varied even within a single cell. Some vesicles were observed undergoing "diffuse-and-go" movement in which diffusional movements in a 0.5 $\mu m^3$ region were interrupted by directional movements over 1 $\mu m$ (Vesicle 1 and 4 in Fig. 7a,b, Vesicle 3 in Fig. 6c, and Vesicle 1 in Supplementary Fig. S1).

Mean square distance (MSD) of vesicles inside neutrophils clearly defined the difference between actively transported phase and diffusive phase (Fig. 6h, Fig. 7e). During the "diffuse" phase, MSD of each vesicle did not increase linearly but reached plateaus (Fig. 6h, and Vesicle 1, 2 and 5 in Fig. 7e). This indicates that the vesicles underwent diffusion in restricted areas, but not in free spaces.

During the "go" phase, the speed of the vesicle reached sometimes 2–4 $\mu m$/sec (Fig. 7c). We measured the velocity of 21 actively transported vesicles in 6 interstitial neutrophils and revealed that the vesicle transports at over 2 $\mu m$/sec were frequently occurred (Supplementary Fig. S2). This is significantly faster than the speed ($\sim$ 1 $\mu m$/sec) of purified molecular motors, such as kinesin or dynein[14].

**Three-dimensional tracking of vesicles in interstitial neutrophils.** To confirm the rapid vesicle transport in the migrating interstitial neutrophils, the 3D movement of vesicles in the neutrophils was analyzed (Fig. 8, Supplementary Movie 6). To track the sequential vesicle position in three dimensions, a scanning session of nine confocal images taken with 1.0 $\mu m$ movements of the objective by the piezoelectric actuator in 1.1 s was repeated 60 times. The focal ($z$) position of the vesicle was determined by fitting the intensity of the fluorescence with a Gaussian curve, as previously described[15]. The 3D movements of vesicles in a single cell were independent of each other, and some vesicles exhibited "diffuse-and-go" movement similar to that observed in 2D (Fig. 7). The 3D speed estimated by this analysis reached a maximum of 3 $\mu m$/sec. We also confirmed
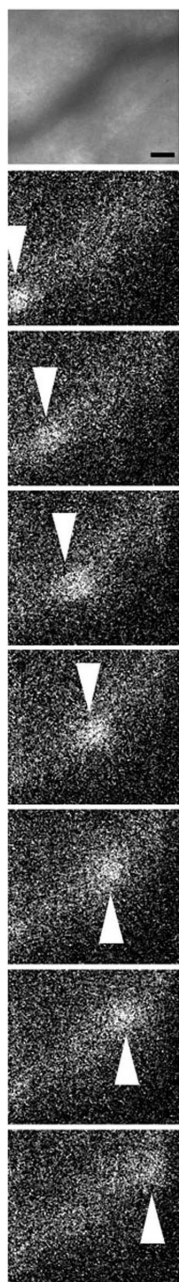
**Figure 3 | Non-invasive observation of neutrophils flowing in the blood vessel.** After the injection of 120 μl of PBS containing 330 nM QDs and 670 nM anti-Ly6G antibody, a blood vessel in the mouse auricle 50 μm below the skin surface was observed following injection of QD-antibody complexes in the absence of inflammation. Transillumination images and fluorescent images were captured (30 msec/frame) at the same position. The transillumination image (upper panel) was averaged over successive ten images. Fluorescent images (other panels) were not averaged. A neutrophil flowing in the vessel is indicated by white arrowheads. The bar indicates 10 μm. A movie of the fluorescent image is available in Supplementary Movie 1.

that the movements of these vesicles took place inside the cell by estimating its cell shape in each continuous confocal images of the vesicles (Supplementary Fig. S3).

## Discussion

In this report, we detail the non-invasive imaging of individual vesicles labeled with QDs in neutrophils located up to 100 μm below the skin surface in the mouse auricle. The improvements in the apparatus, namely a high-power laser and a silicon oil-immersion objective, are essential to viewing QDs in living tissue in which light is strongly scattered and absorbed. Recently, Li et al. developed a new method for non-invasive leukocyte imaging by exciting and detecting the endogenous cellular tryptophan autofluorescence without having to label cells with exogenous fluorescent probes or reporters[16]. This method allowed for the acquisition of images at a video rate (33.3 msec/frame) using a multi-photon microscope coupled with a laser equipped with a β-BBO (beta barium borate) crystal to generate 590 nm pulses. However, using this method, the different types of leukocytes, such as neutrophils, monocytes, and macrophages, could not be easily distinguished. In addition, it is difficult to collect sufficient fluorescence data to visualize internal structures and/or *in vivo* cellular dynamics, which represents a common problem in multi-photon microscopy. In our study, the QD-antibody conjugates were attached specifically to the surface of neutrophils and were endocytosed. Vesicular movement inside the cell was observable. One vesicle appeared to contain many QDs, and the size of the vesicles appeared to correspond to 1 μm beads, indicating that the vesicles were likely phagosomes.

Observations with high spatial and temporal resolution are crucial for detailed analysis of high-speed movement. In our previous studies, the *in vivo* movement of single QD-herceptin conjugates in tumor cells was tracked by the invasive imaging at a video rate (33 ms/frame) with a spatial resolution of 30 nm[7]. The *in vivo* diffusion of single PAR1 on the metastatic tumor cells was also examined at 100 ms/frame with a spatial resolution of 7–9 nm[8]. In the present study, we were able to track vesicular movement within neutrophils non-invasively and *in vivo* with high spatial (15 nm in 2D) and temporal (12.5 ms/frame) resolution (Fig. 2c–f), which corresponds to 5 nm at 100 ms/frame. These measurements are the most accurate among all previously reported *in vivo* imaging studies.

Although understanding the mechanism underlying neutrophil activation is of great biological and physiological significance, the mechanisms controlling vesicular transport have not been well investigated. Rothwell et al. reported that granules within purified human neutrophils moved along paths that corresponded to the radial distribution of microtubules in the cell *in vitro* and that the velocity was 1 to 3 μm/sec[17]. Although they investigated the granule-microtubule interactions in their report, they did not perform any detailed analysis on the movement of the granules. Moreover, the experiments have only been performed using purified neutrophils *in vitro*. To elucidate the mechanisms underlying neutrophil recruitment to the site of inflammation, *in vivo* investigations during neutrophil extravasation are crucial because neutrophil motility is regulated by many microenvironmental factors that may be absent in *in vitro* cultures. Interestingly, we found that vesicular movement in neutrophils adhering to the vascular wall (Fig. 4) was significantly different from the movement of the vesicles in neutrophils moving in the interstitium (Fig. 7). This indicates that inflammatory signals activate not only the interstitial migration of neutrophils but also vesicular transport inside the cell.

Within the neutrophils in the interstitium, some vesicles displayed "diffuse-and-go" movement (e.g., Vesicle 2 and 3 in Fig. 6e; Vesicle 1 and 4 in Fig. 7b, Vesicle 1 and 3 in Fig. 8). Diffusional movements in a volume of approximately 0.5 μm³ were interrupted by directional movements over 1 μm. The viscosity in a purified neutrophil at the trailing region and the cell body was measured to be approximately 0.4 (Pa·s), which is approximately 450-fold greater than that of water[18]. From the relationship between the diffusion constant ($D$) and viscosity ($\eta$) ($D = kT/6\pi\eta r$, where $k$ is the Boltzmann constant, $T$ is temperature and $r$ is size of the vesicle), $D$ is calculated to be $5.7 \times 10^{-15}$ [m²/s] when $T = 37°C$ and $r = 100$ nm. Thus, the diffusion distance in a neutrophil is estimated to be 200 nm in 1 sec. This value is consistent with the vesicle diffusion distance that was observed in
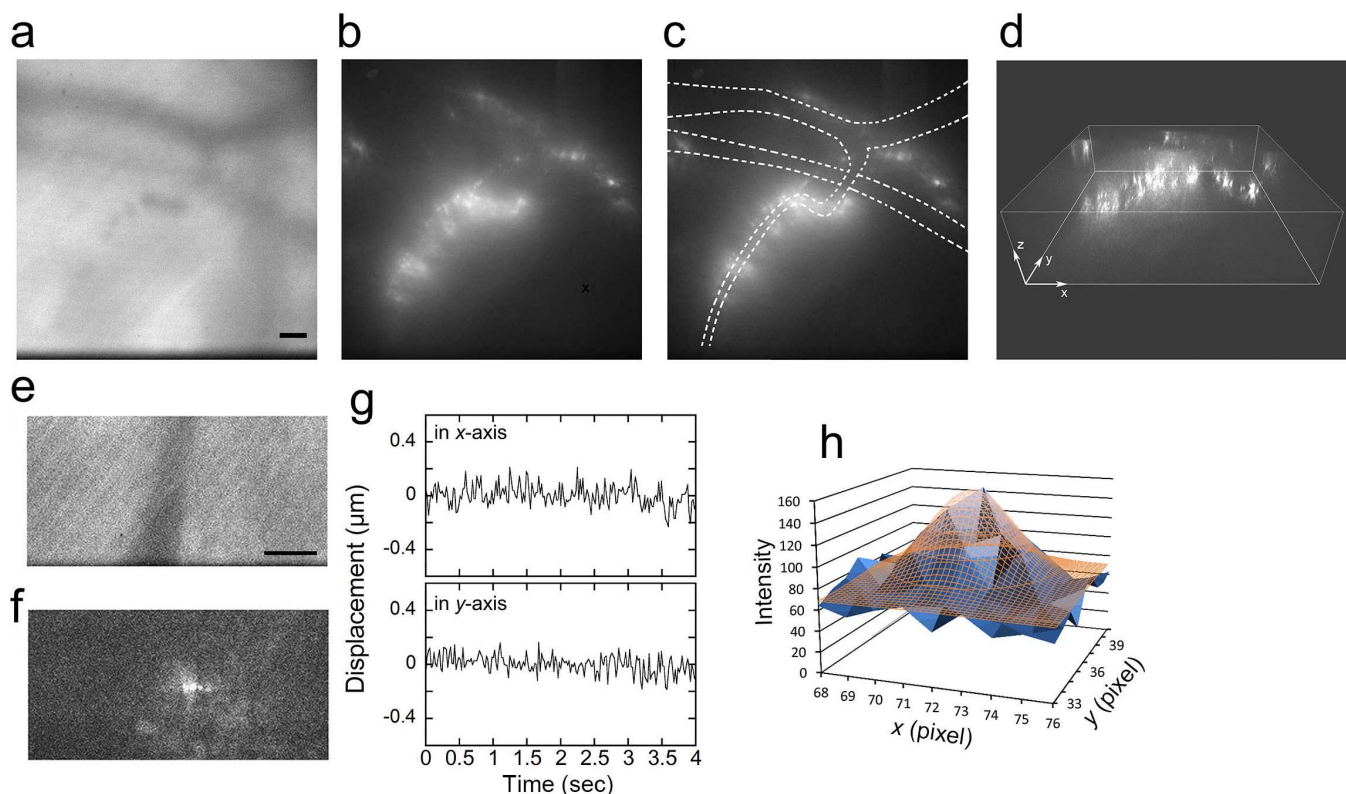
**Figure 4 | Neutrophils forming a cluster around the blood vessel after induction of inflammation.** Inflammation was induced in the mouse auricle via the application of TPA (0.1 mg/ml). (a) A transillumination image of blood vessels at a depth of 70 μm. The images were captured at 30 msec/frame soon after the induction of inflammation and averaged over successive two images. The bar indicates 10 μm. (b–d) By controlling the focal position of the objective with a piezoelectric actuator, a 3D fluorescent image of the neutrophils clustering around the blood vessel was reconstructed. A scanning session of 40 confocal images taken with 1.0-μm movements of the objective in 4.5 s was repeated 5 times. (b) A 2D fluorescent image reconstructed from one set of 40 images. (c) The lumen of the blood vessels was estimated from the transillumination image, which was averaged over successive 50 images, and is represented by broken lines, demonstrating that the neutrophils did not bind to all of the vascular walls. (d) A reconstructed 3D image. Movies of the fluorescent image are available in Supplementary Movies 2 and 3. (e and f) An image of a vesicle within another neutrophil on the vascular wall, 50 μm below the skin surface, was captured at 20 msec/frame, 6 hours after the induction of inflammation. A transillumination image (e) and fluorescent image (f) of the same position were averaged over successive two and five images, respectively. The bar indicates 10 μm. The position of the vesicle was tracked using the FIONA method on the images averaged over successive 5 images (g). The distribution (SD) of the position was 78 nm along the $x$-axis and 69 nm along the $y$-axis. No directional movement was observed. (h) An example of 2D Gaussian fitting to the vesicle by the FIONA method[15]. The intensity of the vesicle (blue solid) was fitted by 2D Gaussian (brown mesh). Center position $(x_0, y_0)$ was (71.68, 37.74) pixels. Width of one pixel corresponds to 223 nm. Other fitting parameters are shown in Supplementary Table S1.

our experiments. Here, we were able to track vesicular movement at 12.5 msec/frame with 15 nm accuracy. The observed diffusional movement (45 nm) of the vesicles was much greater than the noise in our system. Therefore, the diffusional movement of the vesicles was not caused by noise from our experimental system but was independently verified. In our previous study, the QD-trastzumab complexes displayed "stop-and-go" motion in the tumor cell[7]. The increased spatial accuracy in the present study enables us to distinguish the "stop" and "diffuse" motions inside cells. MSD data of

these vesicles indicate that their diffusion did not undergo in free space but in restricted areas (Fig. 6h, Fig. 7e). These vesicles may bind to flexible components of the cytoskeleton, such as actin filaments, or the cytoplasmic environment surrounding the vesicle might be partitioned into sub-micrometer compartments, thereby restricting diffusion. The directions of vesicular transport during the "go" phases preceding and following a "diffuse" phase were often different from each other (Fig. 8). During the "diffuse" phase, vesicles may need to wait to change rails between transport phases.
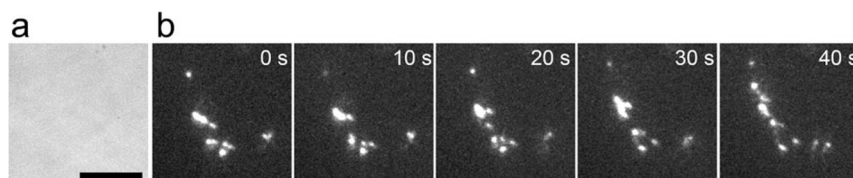


**Figure 5 | Neutrophils migrating in the interstitium.** 24 hours after the induction of inflammation, neutrophils in the interstitium were observed. (a) A transillumination image was taken at 100 msec/frame. No erythrocytes were seen, indicating that interstitium was being observed. (b) At the same position, fluorescent images of a neutrophil with bright vesicles, moving 36 μm below the skin surface, were captured at 100 msec/frame and averaged over successive ten images. The bar indicates 10 μm.
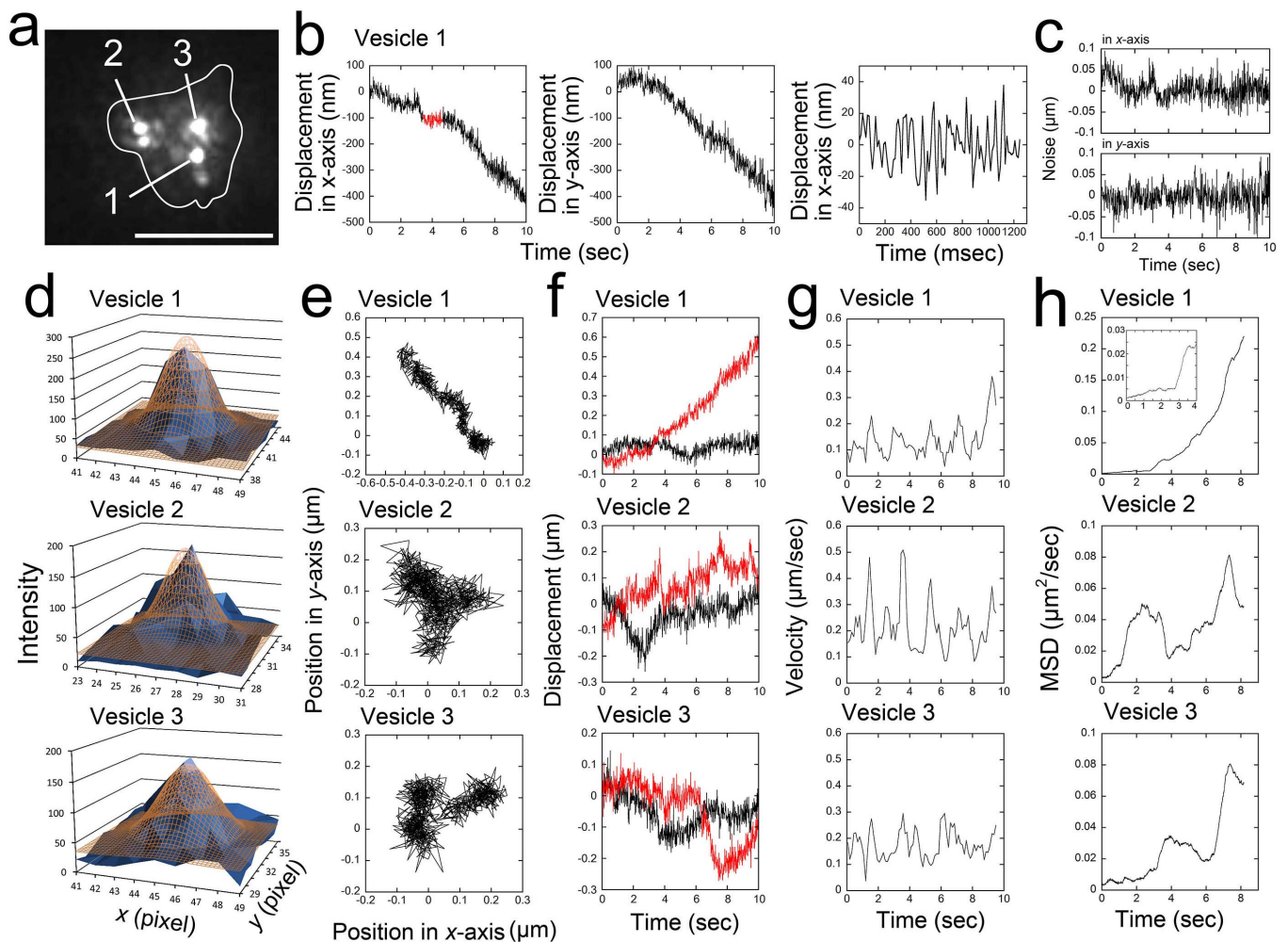
**Figure 6 | High-speed tracking of vesicles within a neutrophil moving in the interstitium.** (a) A fluorescent image of vesicles within a neutrophil in the interstitium at a depth of 32 μm. The images were captured at 12.5 msec/frame, and the image shown was averaged over successive 20 images. The shape of the cell was estimated from the image after averaging over successive 120 images and is indicated by the white line[7]. The bar indicates 10 μm. The vesicles were designated Vesicles 1–3. (b) The displacement of Vesicle 1 relative to the *x*- and *y*- axes. The images were not averaged before tracking. The 3rd figure of (b) shows an enlargement of the displacement to the *x*-axis when the vesicle appeared to stop for 1200 ms on the *x*-axis (shown in red in the leftmost figure of (b)). (c) shows the translocational movement of the Vesicle 1 reduced by 0.3 Hz high-pass filter. (d) The position of the vesicle was tracked using the FIONA method on the non-averaged raw images. The center positions $(x_0, y_0)$ of 2D Gaussian (brown mesh) fitting of the intensity of each vesicle (blue solid) are (44.99, 42.27) pixels for Vesicle 1, (26.61, 33.23) pixels for Vesicle 2, and (45.18, 33.15) pixels for Vesicle 3, respectively. Width of one pixel corresponds to 223 nm. Other fitting parameters are shown in Supplementary Table S1. (e) A 2D trace of each vesicle over 10 seconds. (f) The displacement of each vesicle along the axis rotated relative to vesicle movement. The red line indicates displacements parallel to the rotated axis; the black lines indicate displacements perpendicular to the rotated axis. (g) Velocity of each vesicle. The positions of 10 successive points were averaged, and the speed was calculated from the distance between these two positions. The data were smoothed by taking the moving average of three adjacent points. (h) MSD (mean square distance) of each vesicle. Inset is an enlargement of the MSD at short time.

The movements of vesicles in a single cell appeared to be independent of one another. Although two vesicles were located near each other, one vesicle was selectively transported at high speed, while the other was not (Fig. 7). During the "go" phase, the velocity of the vesicles reached a maximum of 2–4 μm/sec (Fig. 7). During the observation period, the shape of the cell did not seem to change greatly. The maximum locomotion speed of neutrophils in the interstitium is approximately 0.15 μm/sec[6]. Therefore, we postulated that this high-speed vesicle transport is not caused by the locomotive movement of the cell. However, we also recognized that some vesicles moved at a consistently lower speed (approximately 0.1 μm/sec) (e.g., Vesicles 2 and 3 in Fig. 8 and Vesicle 1 in Fig. 6). These vesicles may not be undergoing active transport by molecular motors but rather may be bound to the cytoskeleton of the moving cell.

Influenza viruses in CHO cells were reported to be transported on microtubules with an instantaneous velocity of 1–4 μm/sec at 37°C[19].

Here, high-speed vesicle transport (4 μm/sec) in neutrophils was observed in the auricle at 26°C (± 1°C). The speed of the transport is corrected to ~ 10 μm/sec at 37°C because velocity of motor proteins, kinesin and myosin, which will drive the transport, increased by ~ 2.5 times in increasing temperature from 26 to 37°C[20,21]. Thus the observed vesicular transport in neutrophils was fastest in mammalian cells reported before. Although the molecular basis for the high-speed vesicular transport remains to be defined, there must be a mechanism to transport vesicles at high speeds. One possible mechanism underlying the high-speed vesicular transport is that the actin filaments or microtubules used by molecular motors to transport vesicles are themselves transported by other molecular motors, resulting in the apparent high-speed transport of the vesicle.

The non-invasive imaging using QDs, we developed here, is useful tool to observe the cells and organelles in cells in a mouse and even small animals without changing the physiological conditions. Our
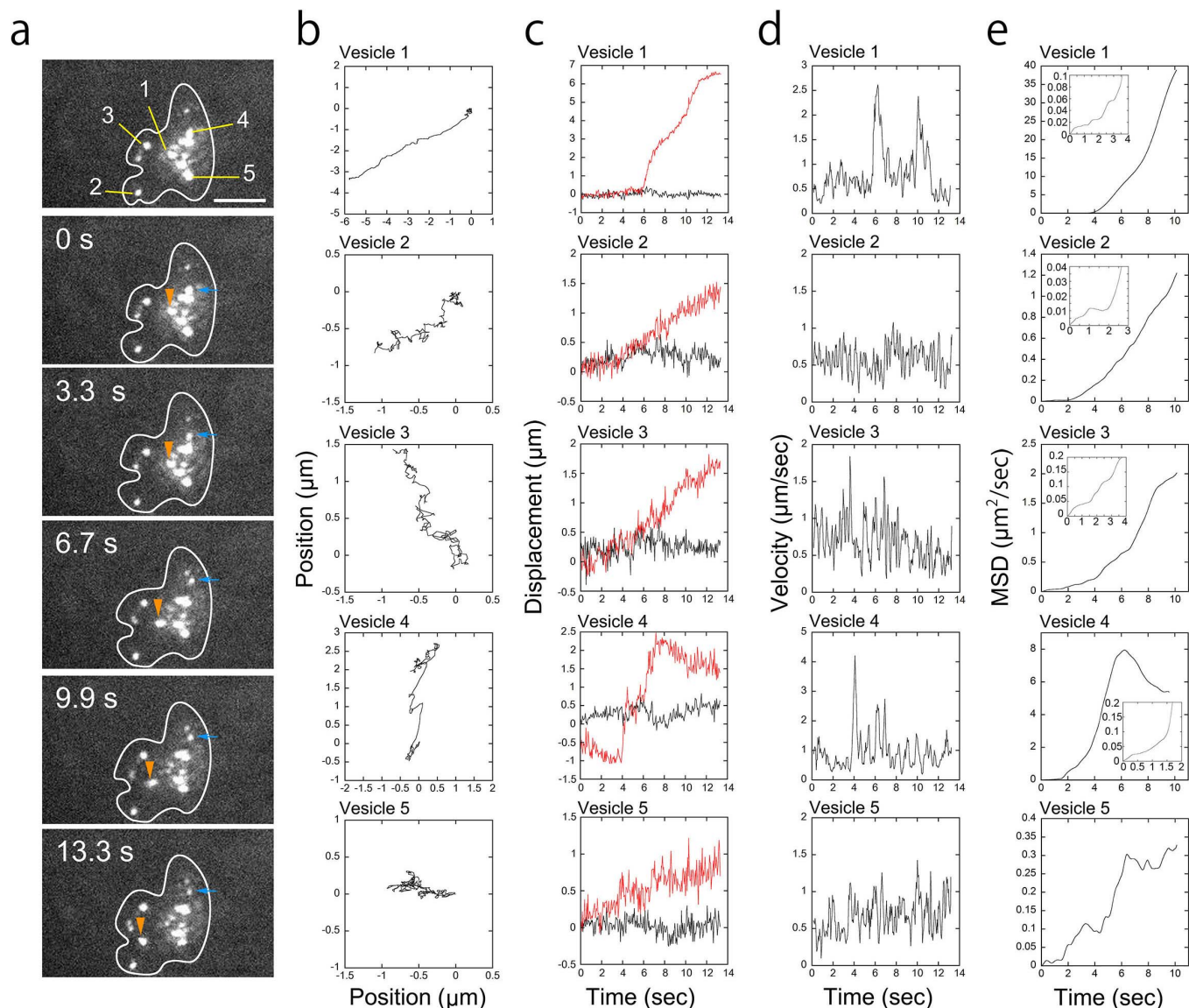
**Figure 7 | High-speed vesicle transport within a neutrophil moving in the interstitium.** (a) Successive fluorescent images of vesicles within a neutrophil moving in the interstitium 50 µm below the skin surface. The images were obtained at 13.3 msec/frame. Each image shown here was averaged over 100 successive images. The bar indicates 10 µm. The vesicles in the cell were designated as Vesicle 1–5. The positions of Vesicle 1 and 4 are indicated by orange and blue arrowheads, respectively. The shape of the cell was estimated from images that were averaged over 250 successive images and is indicated by white lines[7]. (b) Two-dimensional traces of each vesicle over 13.3 seconds. The fluorescent images were averaged four times to get clear images of the vesicles brighter than 40 photons/vesicle, and the two-dimensional trace of each vesicle was tracked using the FIONA method. The fitting parameters are available in Supplementary Table S1. (c) The displacement of each vesicle along the axis rotated relative to the vesicle movement. The red lines indicate displacements parallel to the rotated axis; the black lines indicate displacements perpendicular to the rotated axis. (d) Speed of each vesicle. The positions of 6 successive points were averaged, and the speed of each vesicle was calculated from the distance between these two successive positions. The data were smoothed by taking the moving average of three adjacent points. (e) MSD of each vesicle. Insets are enlargements of the MSDs at short time. A movie of the fluorescent image is available in Supplementary Movie 5.

findings of "diffuse-and-go" and the fast transport of vesicles in activated neutrophils should be important for neutrophil activities. Molecular mechanism of our findings will be revealed near future.

## Methods

**Animals.** Female SCID mice and ddy mice (8 weeks old, weighting 20–27 g) were purchased from Charles River (Yokohama, Japan) and Sankyo Labo Service Corporation (Tokyo, Japan), respectively. All animal experiments were carried out in accordance with the guidelines for animal experiments at the University of Tokyo and were approved by Office for Life Science Research Ethics and Safety in The University of Tokyo.

**Biotinylation of an anti-neutrophil antibody.** A monoclonal anti-mouse Ly6G antibody (R&D Systems) was biotinylated by incubation with Biotin-OSu (AnaSpec) and purified over a Sephadex G-25 column.

**Optical system with spinning-disk confocal microscopy.** The optical system used for the non-invasive observation of the QDs in the mouse auricle was essentially the same system described in our previous study, with modifications[7]. The system consisted of an inverted-epifluorescence microscope (IX71, Olympus) equipped with a silicon oil-immersion objective (NA: 1.3, UPLSAPO 60 × S, Olympus), a spinning-disk confocal system (CSU-22, Yokogawa) and an EMCCD camera (iXon DU-897E, Andor) (Fig. 2a).

Blood vessels in the mouse auricle were visualized via transillumination with blue light obtained from filtering halogen light through a 400–440 nm band-pass filter. The blood vessels were imaged on an EMCCD camera through the confocal system. QDs in the auricle were illuminated by epifluorescence illumination using a green laser (532 nm, 500 mW, JUNO) expanded by convex and concave lenses. A shutter (F116, Suruga-Seiki, Japan) was located next to the laser. The intensity of the laser was regulated by neutral density filters (Transmittance with 1, 5, 10, 30, 50%, Sigma, Japan) mounted on a motorized filter wheel (FW103, Tholabs). The fluorescence
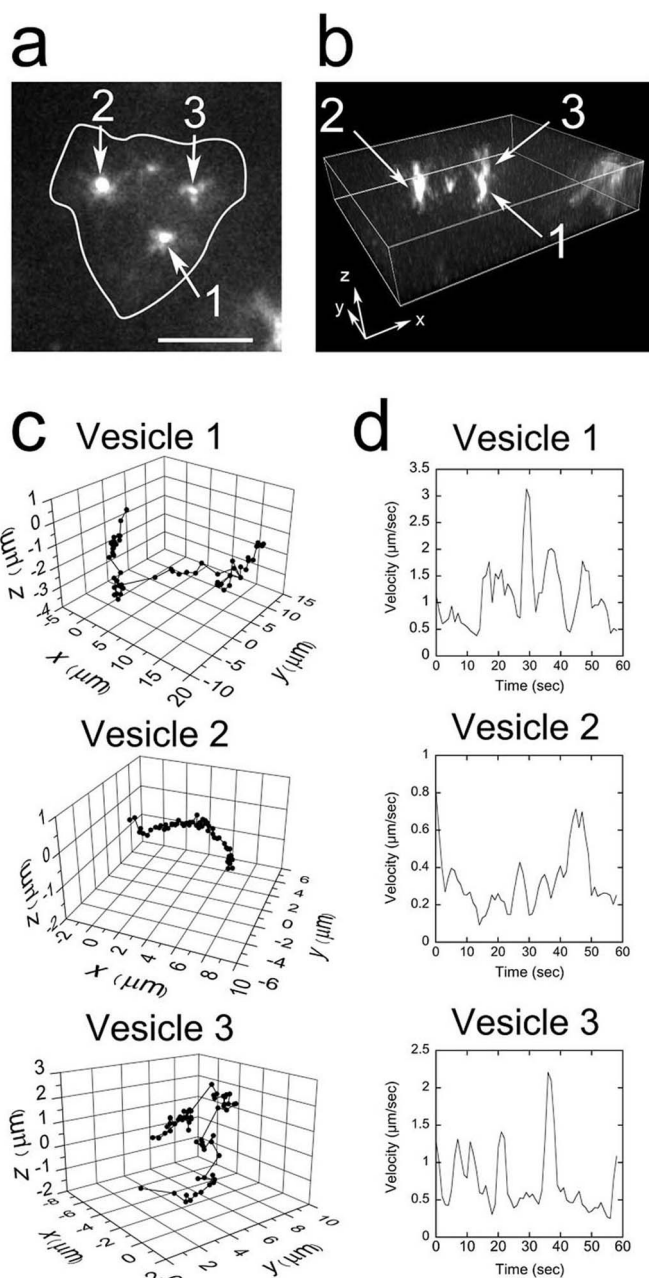
**Figure 8 | Three-dimensional tracking of vesicles within neutrophils in the interstitium.** A scanning session of nine confocal images taken with 1.0-μm movements of the objective in 1.1 s was repeated 60 times, allowing for the 3D tracking of the vesicle positions within a given cell 45 μm below the skin surface. (a) A fluorescent 2D image of the neutrophil. One set of nine confocal images was averaged. The bar indicates 10 μm. The vesicles in the cell were designated as Vesicle 1–3. (b) A reconstructed 3D image. The depth of the image was 9 μm. (c) Three-dimensional tracking of three vesicles. The focal (z) position of the vesicle was determined by fitting the intensity of the fluorescence with a Gaussian curve[15]. (d) The speeds of the vesicles. The data were smoothed by taking the moving average of three adjacent points. A movie of the fluorescent image is available in Supplementary Movie 6.

from QDs was filtered with a 685–725 nm band-pass filter (Chroma) in front of the EMCCD camera. Images of the QDs were normally captured at 33.3 msec/frame (30 frames/sec) and the rotation speed of the spinning-disk of the CSU system was set at 1800 rpm. When the rapid movement of vesicles in the neutrophil was measured, images were obtained at 12.5 ms/frame (80 frames/sec), and the rotation speed of the spinning-disk was increased to 4800 rpm. Some images shown in this article were averaged to obtain clear images as needed. The z-position of the objective was

controlled by a piezoelectric actuator with an electrostatic capacity sensor (PI, Germany), which enabled us to obtain three-dimensional images.

**Purification of leukocytes and subsequent labeling with QD/antibody conjugates.** Two milliliters of phosphate-buffered saline (PBS) containing 20 mg/ml casein (MP Biomedical) was injected into the peritoneal cavity of ddY mice two times: 12 hours and 3 hours before the harvest. Mice were euthanized by isoflurane asphyxiation and peritoneal fluid was collected with 10 ml of PBS. Between $10^7$ and $10^8$ leukocytes were routinely harvested. The peritoneal fluid was centrifuged at $200 \times g$ for 10 min to obtain purified leukocytes.

Streptavidin-conjugated QDs (330 nM) (Qdot 705 Streptavidin Conjugate, Invitrogen) were mixed with the biotinylated anti-Ly6G antibody (670 nM) for 30 min at room temperature (24°C). The harvested leukocytes were incubated on ice with various concentrations of QDs (1–20 nM) and anti-Ly6G antibody (2–40 nM) and then washed three times with 10 ml PBS to eliminate any unbound QDs. Both transillumination and fluorescent images of the QD-labeled neutrophils were taken using the confocal microscope system described above.

**Non-invasive imaging of neutrophils labeled with QDs in the mouse auricle.** Mice were anesthetized with 1–3% isoflurane on the stage of the microscope. The room temperature was kept at 24 ± 1°C. The temperature in the auricles was measured to be 26° ± 1°C by a thin thermocouple inserted in the auricles (HFT-50, Anritsu, Japan). Hair was removed from a SCID mouse auricle using a depilatory cream (Hydro'Restor Hair Removal Cream, Veet) for 5 min. Then, the cream was washed out by 70% ethanol. When depilatory cream alone was applied, we observed that the neutrophils attached to the vascular wall (Supplementary Fig. S4), suggesting that the removal of hair using the depilatory cream may also induce inflammatory signals. However, the inflammation lasted only for a short time, and we could not recognize it on the following day. Inflammation was induced by the application of 20 μl of 12-O-tetradecanoylphorbol 13-acetate (TPA; 0.1 mg/ml in acetone, Wako, Japan) on the auricle epidermis. The auricle was placed between two glass coverslips with 50% paraffin and 50% vaseline as an adhesive and firmly fixed to the stage by adhesive tape in order to remove the oscillation caused by the heartbeat and respiration (Fig. 2b).

The biotinylated anti-Ly6G antibody (170–670 nM) was incubated with streptavidin coated QDs (83–330 nM) in 120 μl of PBS for 30 min at room temperature. The QD-anti-Ly6G antibody conjugate in the resulting solution was injected into the tail vein of female SCID mice. The final concentration of the QDs in the mouse blood was estimated to be 5–20 nM.

We took care to shut off the laser illumination when it was not needed to avoid damage from the high intensity of the laser. After the appropriate observations were made, the mice were euthanized with excess isoflurane anesthesia. However, they could also survive in a healthy state for over a month following the injection of QDs and the observation. Red swelling of the ears as a result of the laser illumination was not observed. We did not assess the damage of the experiments over a longer period of time.

**Analysis of QD movement.** The two-dimensional position of the QDs in the mouse auricle was tracked using the FIONA method that was used in our previous experiments[15]. The fitting parameters are shown in Supplementary Table S1. Sometimes images of vesicles were not bright enough to track by the FIONA method, because the neutrophil migrated deep from the skin surface or the vesicles contained only small number of QDs. In this case, we averaged over successive images in order to make the vesicles brighter than 40 photons/vesicle, although spatial precision was increased by sacrificing temporal resolution. The temporal resolution of averaged displacement data in Fig. 4, 7 and 8 is calculated from (time/frame) × (number of averaged frames).

For estimating the effect of averaging over the successive images on the vesicle displacement, we compared the displacement from the raw non-averaged images and that from the averaged images (Supplementary Fig. S5). The trace from averaged data was completely superimposed with that from the original non-averaged data with smaller noise, indicating that the averaging operation does not affect the net displacement of the vesicles but reduces the noise of the movement.

We are able to calculate the localization accuracy theoretically from the equation[22], $\sqrt{\dfrac{\sigma^2}{N} + \dfrac{a^2}{12N} + \dfrac{8\pi\sigma^4 b^2}{a^2 N^2}}$, where notations are the number of photons ($N$), standard deviation ($\sigma$) of the Gaussian, pixel size ($a$) and standard deviation ($b$) of background intensity noise. The theoretical accuracy was calculated to be 8.3 nm in Vesicle 1 (Fig. 6) at the values of $N = 1620$, $\sigma_x = 268$ (nm), $a = 223$ (nm) and $b = \sqrt{22}$. The theoretical accuracy (8.3 nm) is much smaller than the experimental one (> 15 nm). Therefore, the experimental accuracy including noises came from apparatus and the movements of mouse respiration and heart beat is practically more important in our measurements.

When we measured the translocational speeds of vesicles, we further average the data of displacement to reduce velocity error (or S.D. of velocity noise) which was derived from the calculation of displacement noise divided by time. For example, displacement noise (15 nm) divided by time (12.5 msec) in Fig. 6 gives large noise in velocity (1.2 μm/sec). To reduce the velocity noise, we averaged over 30 frames in Fig. 6 and got displacement of ~ 3 nm. The velocity noise was calculated to be 3 nm/(12.5 msec X 30) = 8 nm/sec, which is negligibly small. In all of the velocity data, we averaged over the displacement data to reduce the velocity noise < ~ 20 nm/sec so that the velocities were accurately determined.

The focal (z) position of the QDs was determined by fitting the intensity of the QD fluorescence with a Gaussian curve as previously described[15].

1. Witko-Sarsat, V., Rieu, P., Descamps-Latscha, B., Lesavre, P. & Halbwachs-Mecarelli, L. Neutrophils: molecules, functions and pathophysiological aspects. *Lab. Invest.* **80**, 617–653 (2000).
2. Amulic, B., Cazalet, C., Hayes, G. L., Metzler, K. D. & Zychlinsky, A. Neutrophil function: from mechanisms to disease. *Annu. Rev. Immunol.* **30**, 459–489 (2012).
3. Borregaard, N. Neutrophils, from marrow to microbes. *Immunity* **33**, 657–670 (2010).
4. Faust, N., Varas, F., Kelly, L. M., Heck, S. & Graf, T. Insertion of enhanced green fluorescent protein into the lysozyme gene creates mice with green fluorescent granulocytes and macrophages. *Blood* **96**, 719–726 (2000).
5. Chtanova, T. *et al.* Dynamics of neutrophil migration in lymph nodes during infection. *Immunity* **29**, 487–496 (2008).
6. Kreisel, D. *et al.* In vivo two-photon imaging reveals monocyte-dependent neutrophil extravasation during pulmonary inflammation. *Proc. Natl Acad. Sci. U. S. A.* **107**, 18073–18078 (2010).
7. Tada, H., Higuchi, H., Wanatabe, T. M. & Ohuchi, N. In vivo real-time tracking of single quantum dots conjugated with monoclonal anti-HER2 antibody in tumors of mice. *Cancer Res.* **67**, 1138–1144 (2007).
8. Gonda, K., Watanabe, T. M., Ohuchi, N. & Higuchi, H. In vivo nano-imaging of membrane dynamics in metastatic tumor cells using quantum dots. *J. Biol. Chem.* **285**, 2750–2757 (2010).
9. Hamada, Y. *et al.* In vivo imaging of the molecular distribution of the VEGF receptor during angiogenesis in a mouse model of ischemia. *Blood* **118**, e93–e100 (2011).
10. Michalet, X. *et al.* Quantum dots for live cells, in vivo imaging, and diagnostics. *Science* **307**, 538–544 (2005).
11. Fleming, T. J., Fleming, M. L. & Malek, T. R. Selective expression of Ly-6G on myeloid lineage cells in mouse bone marrow. RB6-8C5 mAb to granulocyte-differentiation antigen (Gr-1) detects members of the Ly-6 family. *J. Immunol.* **151**, 2399–2408 (1993).
12. Lämmermann, T. *et al.* Rapid leukocyte migration by integrin-independent flowing and squeezing. *Nature* **453**, 51–55 (2008).
13. Friedl, P. & Weigelin, B. Interstitial leukocyte migration and immune function. *Nat. Immunol.* **9**, 960–969 (2008).
14. Toba, S., Watanabe, T. M., Yamaguchi-Okimoto, L., Toyoshima, Y. Y. & Higuchi, H. Overlapping hand-over-hand mechanism of single molecular motility of cytoplasmic dynein. *Proc. Natl Acad. Sci. U. S. A.* **103**, 5741–5745 (2006).
15. Watanabe, T. M. & Higuchi, H. Stepwise movements in vesicle transport of HER2 by motor proteins in living cells. *Biophys. J.* **92**, 4109–4120 (2007).
16. Li, C. *et al.* Imaging leukocyte trafficking in vivo with two-photon-excited endogenous tryptophan fluorescence. *Opt. Express* **18**, 988–999 (2010).
17. Rothwell, S. W., Nath, J. & Wright, D. G. Interactions of cytoplasmic granules with microtubules in human neutrophils. *J. Cell Biol.* **108**, 2313–2326 (1989).
18. Yanai, M. *et al.* Intracellular elasticity and viscosity in the body, leading, and trailing regions of locomoting neutrophils. *Am. J. Physiol.* **277**, C432–C440 (1999).
19. Lakadamyali, M., Rust, M. J., Babcock, H. P. & Zhuang, X. Visualizing infection of individual influenza viruses. *Proc. Natl Acad. Sci. U. S. A.* **100**, 9280–9285 (2003).
20. Kawaguchi, K. & Ishiwata, S. Thermal activation of single kinesin molecules with temperature pulse microscopy. *Cell Motil. Cytoskeleton* **49**, 41–47 (2001).
21. Rossi, R., Maffei, M., Bottinelli, R. & Canepari, M. Temperature dependence of speed of actin filaments propelled by slow and fast skeletal myosin isoforms. *J. Appl. Physiol.* **99**, 2239–2245 (2005).
22. Thompson, R. E., Larson, D. R. & Webb, W. W. Precise nanometer localization analysis for individual fluorescent probes. *Biophys. J.* **82**, 2775–2783 (2002).

## Acknowledgements

## Author contributions

All authors designed experiments. K.K. and S.K. performed experiments, K.K. and H.H. analysed data, and K.K. and H.H. wrote the paper. All authors read and approved the manuscript.

## Additional information

**How to cite this article:** Kikushima, K., Kita, S. & Higuchi, H. A non-invasive imaging for the *in vivo* tracking of high-speed vesicle transport in mouse neutrophils. *Sci. Rep.* **3**, 1913; DOI:10.1038/srep01913 (2013).